Mecánica Computacional Vol. XXI, pp. 2343–2360
S. R. Idelsohn, V. E. Sonzogni and A. Cardona (Eds.)
Santa Fe–Paraná, Argentina, October 2002

PARALLEL FINITE ELEMENT MODEL FOR SURFACE AND SUBSURFACE HYDROLOGY

Rodrigo R. PAZ†, Mario A. STORTI†, Sergio R. IDELSOHN†, Leticia B. RODRIGUEZ*, Carlos A. VIONNET* and Germán P. FARIAS*

†Centro Internacional de Métodos Computacionales en Ingeniería (CIMEC)
Universidad Nacional del Litoral, CONICET.
Güemes 3450. 3000 Santa Fe. Argentina.
e-mail: rodrigop@intec.unl.edu.ar, url: http://venus.ceride.gov.ar/cimec

*Grupo de Estudios Hidro-Ambientales (GEHA).
Universidad Nacional del Litoral, CONICET.
Paraje El Pozo, 3000 Santa Fe, Argentina.
e-mail: vionnet@fich1.unl.edu.ar

Key Words: finite element method, parallel computing, hydrology, surface and subsurface flow.

Abstract. *The large spread in length scales present in the hydrological problems requires a high degree of refinement in the finite element mesh and, then, requires very large computational resources. Also, in a 2D multi-aquifer model, the number of unknowns per surface node is, at least, equal to the number of aquifers and aquitards. Due to this fact, it is expected to have a very high demand of CPU computation time, calling for parallel processing techniques. A C++ FEM code based on the PETSc-FEM and PETSc libraries was developed.*

Several systems of aquifers/aquitards coupled with a net of surface streams can be solved. The streams are modeled with the KWM (Kinematic Wave Model) approximation and there is mass exchange between streams and aquifers through a resistance coefficient at the stream walls. Both Manning and Chèzy friction models are available for the streams.

1 INTRODUCTION

The aim of this work is to present the state of development of Large Scale Model for Surface and Subsurface water flow in multi-aquifer systems. The study area is the argentinian Litoral, in the middle north-east of the country, where several non connected multi-aquifer/river systems are founds (i.e Cululú, Las Conchas, San Antonio, Colastiné and Monjes-Cañada Carrizales drainage systems), (Fig. 1). This area represents 1/8 of the total area of the province of Santa Fe (130.000 km^2).

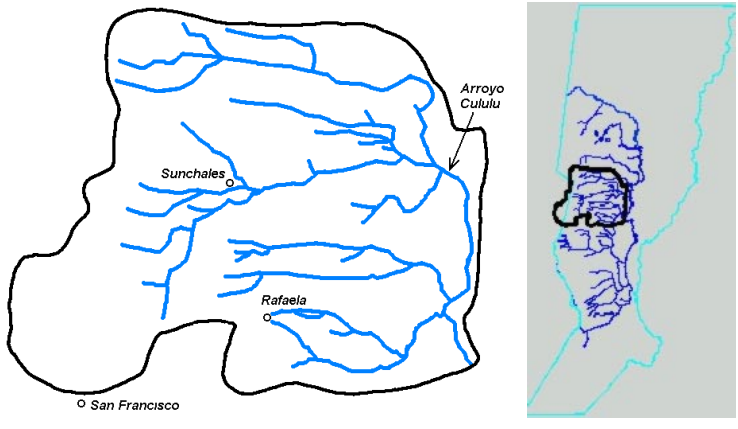

Figure 1: Drainage network and system location in province of Santa Fe.

Surface and subsurface water flow problems (i.e. multi-aquifer/river systems) deal with coupled nonlinear and linear differential equations in complex domains and dissimilar time scales. The problem is highly dependent of the terrain topology where water flows. We present the manner to obtain a "good" Delaunay tesellation from satellite data images and the DTM data, digital terrain model (obtained from 88 topographical maps, scale 1:50.000), which represents the geometry of the stream/aquifer system and therefore the mesh for the parallel finite element model. We interpolate any system physical properties or via the Natural Neighbor Method.
The mathematical treatment of ground-water flows follows the confined aquifer theory or the classical Dupuit approximation for unconfined aquifers whereas surface-water flows are treated with the kinematic wave approximation for open channel flow (KWM model) as a first approximation and we expect to implement a 2D Saint-Venant model in subsequent step. A mathematical expression similar to Ohm's law is used to simulate the interacting term among the two hydrological components. The spread in time (slow time scale for ground-water flow and fast time scale for surface flow) and length scales requires an important degree of refinement in drainage network neighborhoods.

2 THE HYDROLOGICAL MODEL

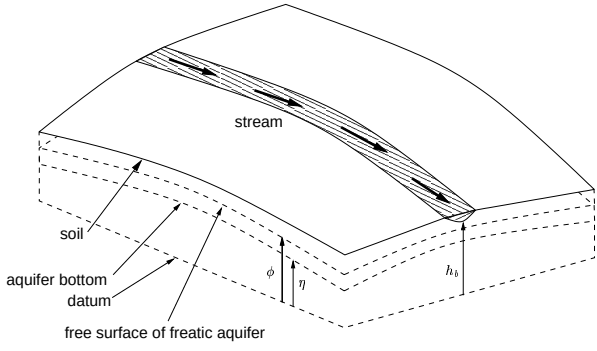

Figure 2: Aquifer/stream system.

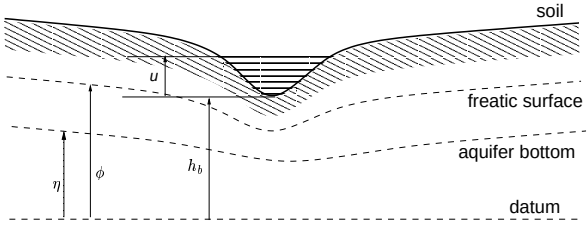

Figure 3: Aquifer/stream system. Transverse 2D view.

The implemented module solves the problem of subsurface flow in a free aquifer, coupled with a surface net of 1D streams. To model such system three element sets must be used: an `aquifer` system representing the subsurface aquifer, a `stream` element set representing the 1D stream and a `stream_loss` element set representing the losses from the stream to the aquifer (or vice versa) see Fig. 2 and Fig. 3.

The `aquifer` element set is a 2D element set with triangle or quadrangle elements (see Fig. 4). A per-node property `eta` represents the height of the aquifer bottom to a given datum. The corresponding unknown for each node is the piezometric height or the level of the freatic surface at that point ϕ. On the other hand, the `stream` element set represents a 1D stream of water. It has its own nodes, separate from the aquifer nodes, whose coordinates must coincide with some corresponding node in the aquifer. For instance, the aquifer element in the figure is connected to nodes $n1$, $n2$ and $n3$, while the

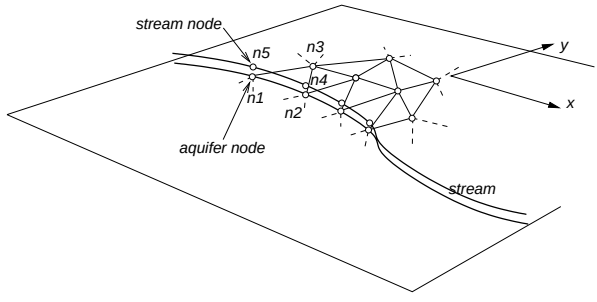

Figure 4: Aquifer/stream system. Discretization.

stream element is connected to nodes $n4$ and $n5$. $n1$ and $n4$ have the same coordinates (but different unknowns) and also $n2$ and $n5$. A constant per node field represents the stream bottom height h_b, with reference to the datum. So that, normally, we have for each node two coordinates and the stream bottom height. The unknown for these nodes is the height u of the stream free water surface with reference to the stream bottom. The channel shape and friction model and coefficients are entered via properties described below. If the stream level is above the freatic aquifer level ($h_b + u > \phi$) then the stream losses water to the aquifer and vice versa.

The equation for the aquifer integrated in the vertical direction is

$$\frac{\partial}{\partial t}\left(S(\phi - \eta)\phi\right) = \nabla \cdot (K(\phi - \eta)\nabla\phi) + \sum G_a, \tag{1}$$

where S is the storativity, K is the hydraulic conductivity and G is a source term, due to rain, losses from streams or other aquifers.

The equation for the stream is, according to the *"Kinematic Wave Model" KWM* approach,[1]

$$\frac{\partial A(u)}{\partial t} + \frac{\partial Q(A(u))}{\partial s} = G_s, \tag{2}$$

where u is the unknown field that represents the height of the water in the channel with respect to the channel bottom as a function of time and a linear arc coordinate along the stream, A is the transverse cross section of the stream and depends, through the geometry of the channel, on the channel water height u. Q is the flow rate and, under the KWM model is a function only of A through the friction law.

$$Q = \gamma A^m, \tag{3}$$

where $\gamma = C_h\, S^{1/2}\, P^{-1}$ and $m = 3/2$ for the Chèzy friction model, and $\gamma = \bar{a}\, n^{-1}\, S^{1/2}\, P^{-2/3}$ and $m = 5/3$ for the Manning model, where $S = (\mathrm{d}h_b/\mathrm{d}s)$ is the slope of the stream bottom, P is the wetted perimeter, and C_h, $\bar{a}$ and n (the Manning roughness) are model

constants.
The stream/aquifer interaction process occurs between a stream and its adjacent flood-plain aquifer. Then, we can write the coupling,

$$G_s = P/R_f(\phi - h_b - u), \tag{4}$$

where G_s represent the gain or loss of the stream, and the main component is the loss to the aquifer and R_f is the resistivity factor per unit arc length of the perimeter. The corresponding gain to the aquifer is

$$G_a = -G_s\,\delta_{\Gamma_s}, \tag{5}$$

where Γ_s represents the planar curve of the stream and δ_{Γ_s} is a Dirac's delta distribution with a unit intensity per unit length, i.e.

$$\int f(\mathbf{x})\,\delta_{\Gamma_s}\,\mathrm{d}\Sigma = \int_0^L f(\mathbf{x}(s))\,\mathrm{d}s. \tag{6}$$

The `stream_loss` element set represents this loss, and a typical discretization is shown in Fig. 4. The stream loss element is connected to two nodes on the stream and two on the aquifer.
Contrary to standard approaches, the coupling term is incorporated through a boundary flux integral that arises naturally in the weak form of the governing equations rather than through a source term.

3 NATURAL NEIGHBOR INTERPOLATION

In order to interpolate physical properties and topographical data from DTM maps we have implemented a C++ Natural Neighbor interpolation function using CGAL geometrical library[2](http://www.cgal.com/).
Natural Neighbor shape functions are C^∞ everywhere, except at the nodes where they are C^0 ([3]), see Fig. 5. This property and properties showed below make them powerful in order to obtain a smooth interpolation.
Let $\mathbf{x} \in \Omega \subset R^n$ be a point in R^n (n: the space dimension). Consider an interpolation scheme for a vector-valued function (or a vector-field) $u(\mathbf{x}) : \Omega \to R^n$,

$$u^h(\mathbf{x}) = \sum_{i=1}^{N} \phi_i(\mathbf{x}) u_i, \tag{7}$$

where $u_i (i = 1, 2, ..., N)$ are the nodal values at the N natural neighbors, and ϕ_i are the natural neighbors shape functions associated with each node. For $n = 2$ the shape function for the node i is the ratio of the area of overlap of the $2^{nd} order$ dual Delaunay

tessellation cells[4] (i.e $2^{nd}order$ Voronoi diagram cells) to the total area of the Voronoi cell of $\mathbf{x}$, (see Fig. 6 and Fig. 7).

$$\phi_i(\mathbf{x}) = \frac{A_i(\mathbf{x})}{A(\mathbf{x})}, \tag{8}$$

where $A(\mathbf{x}) = \sum_{j=1}^{N} A_j(\mathbf{x})$. For instance, the shape function for node 3 is

$$\phi_3(\mathbf{x}) = \frac{A_3(\mathbf{x})}{A(\mathbf{x})}. \tag{9}$$

3.1 Properties

3.1.1 Interpolation

By definition of the shape function, Eq. 8), the property $0 \leq \phi_i(\mathbf{x}) \leq 1$ is evident. If $\mathbf{x}$ coincide with any node, i. e. with node i, then it is seen that $\phi_i(\mathbf{x}) = 1$ and $\phi_j(\mathbf{x}) = 0 \; \forall j \neq i$. Then,

$$\phi_i(\mathbf{x}_j) = \delta_{ij}. \tag{10}$$

3.1.2 Partition Unity

From Eq. 8, we have

$$\sum_{i=1}^{N} \phi_i(\mathbf{x}) = 1 \;\; in \; \Omega. \tag{11}$$

This relation implies that the interpolant exactly reproduce constant functions.

3.1.3 Linear Completeness

Natural Neighbors shape functions also satisfy local coordinate property,

$$\mathbf{x} = \sum_{i=1}^{N} \phi_i(\mathbf{x})\mathbf{x}_i, \tag{12}$$

then, this interpolant function can exactly reproduce the geometrical coordinates.

3.1.4 Support

The support is seen to be the union of Delaunay circumcircles about node A (see Fig. 5).

The interpolation algorithm proceeds as follows:

1. Construct a Delaunay tessellation with nodes where values are knowns

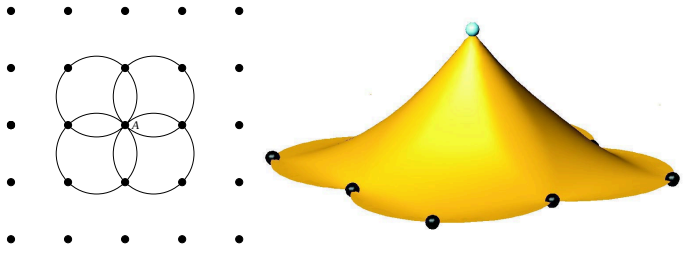

Figure 5: Support and Natural Neighbor shape function.

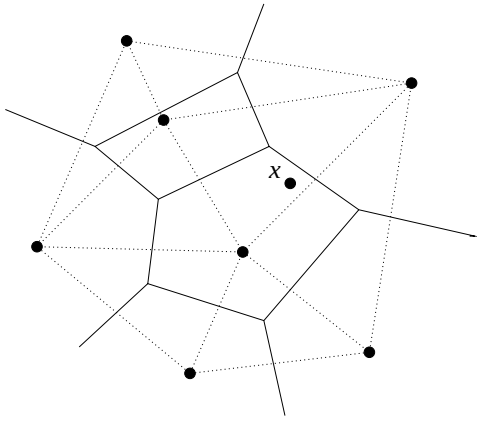

Figure 6: 1^{st}*order* voronoi diagram.

2. For each node n_i where we wish know the vector-value $u^h(\mathbf{x})$
   - Find the face F_{n_i} such as $n_i \in F_{n_i}$
   - Construct a secondary local Delaunay tessellation with nodes in F_{n_i} and node n_i
   - Compute $A_i(\mathbf{x}), \quad (i = 1, 2, ..., N)$
   - Compute $u^h(\mathbf{x})$ with Eq. 7

For instance, we can see in Fig. 8 points the height interpolation for nodal point of a refined triangulation for our stream/aquifer FEM application (in black) from from iso-height data points DTM map (in red) using the algorithm above.

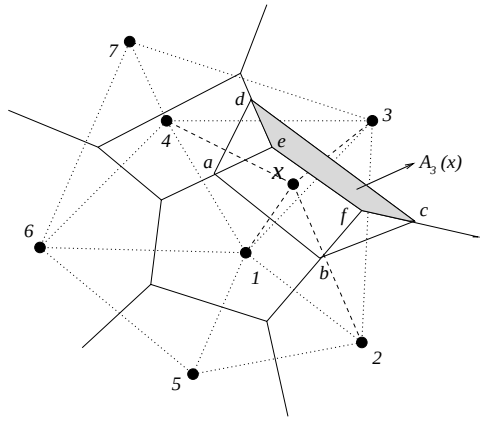

Figure 7: $2^{nd}order$ voronoi diagram for $\mathbf{x}$.

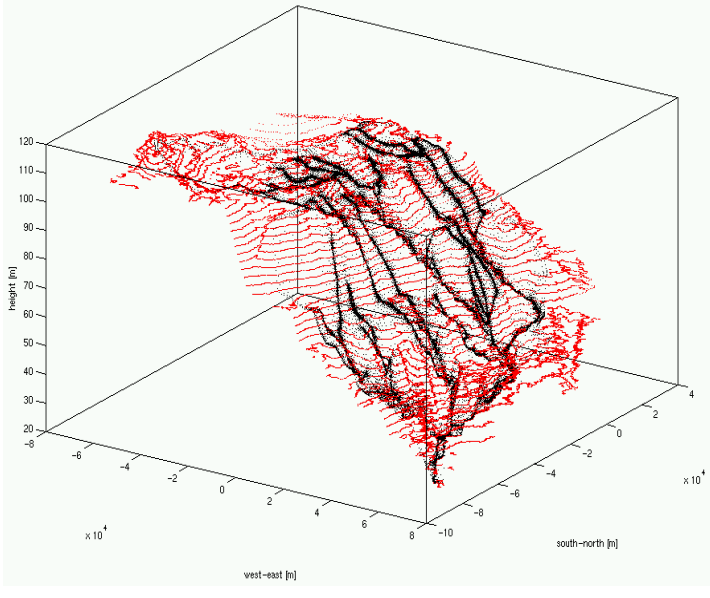

Figure 8: Height interpolation.

4 FEM COMPUTATIONS

The large time and length scales presents in surface-water and ground-water flow problems entails to a large demand of computational resources. Typically, the range of length scales vary among hundred of kilometers and hundred of meters while time scale vary between days and years. A rough estimate suggests that triangulations in the order of 100,000 to 1,000,000 triangles should be used. Moreover, considering multi-aquifer system with several layers the number of unknowns will be 10 to 20 unknowns per node. Therefore, the expected number of unknowns lie between 10^6 and 10^7.
Regarding the efficiency of parallelism, FEM computations can be split basically in two parts, matrix and right hand side assembly and linear system solution. The right hand side and the matrix can be assembled in each processor almost independently, at the exception of the contribution to nodes in the inter-subdomain interfaces. This requires some inter-processor communication, but this is usually irrelevant, specially for very large problems (In fact, the relation communication/computation for the assembly stage and for a given fixed problem, scales with h, the mesh size.) The solution stage requires more communication and, then, is less parallelizable. The strategy used in this work is to use a Domain Decomposition Method, i.e. a mixture of iterative and direct solvers. We iterate a GMRES method on the interface,[5–10] and solve with a LU factorization in the subdomain interiors. With this strategy, high computational efficiency can be attained. We adopt a Backward Euler scheme for time integration.

5 NUMERICAL RESULTS

We present two examples of surface and subsurface interaction flow for Cululú stream system. The first example is periodic case with wet and dry seasons (Fig. 9). A wet season of 200 days with a precipitation rate of 1,000 mm/year. introduced in wet periods is the annual average precipitation observed in last years (1,000 mm/year). A mesh of 96,131 triangular elements and 48,452 nodal points is used to represent the aquifer domain (see Fig. 10). The average space between nodal river points is 100 meters. At time $t = 0$ the piezometric height in freatic aquifer is 30 meters above the aquifer bottom, while the water height in stream is 10 meters above the streambed.
The hydraulic conductivity and storativity of freatic aquifer are $2 \cdot 10^{-3}$ and $2.5 \cdot 10^{-2}$, respectively. We adopt the Manning friction law. The roughness of stream channel is $3 \cdot 10^{-3}$ and the river width is 10 meters. The `stream_loss` resistivity average value is 10^5. The time step adopted in both cases is $Dt = 1$ day.
The time used to solve each time step in the nonlinear coupled problem with 7 processor Pentium IV 1.4-1.7 Ghz and 512 Mb RAM (Rambus) connected through a switch Fast Ethernet (100 Mbit/sec, latency=$O(100)$) was 3.6 seconds in average.

5.1 First case

In figures 11 to 17 we see the freatic height level at time stages showed in Fig. 9.
The slightly increment in freatic levels in river vicinities is due to the high value of R_f.
This value is not well determined yet and is the higher expected for that stream system.

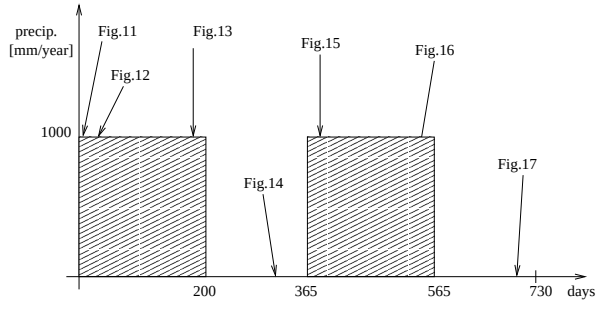

Figure 9: Rain periods.

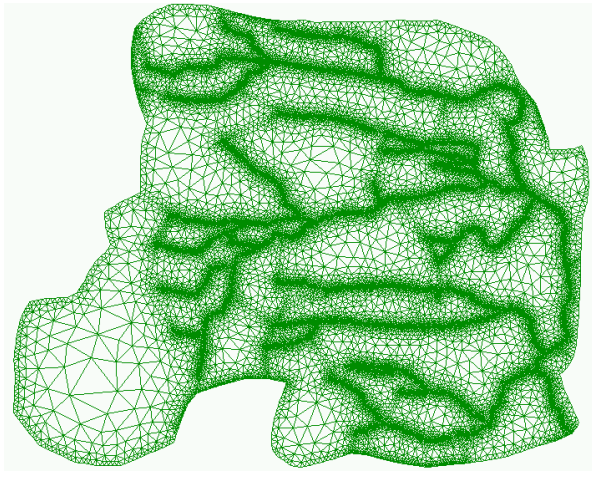

Figure 10: Aquifer mesh.

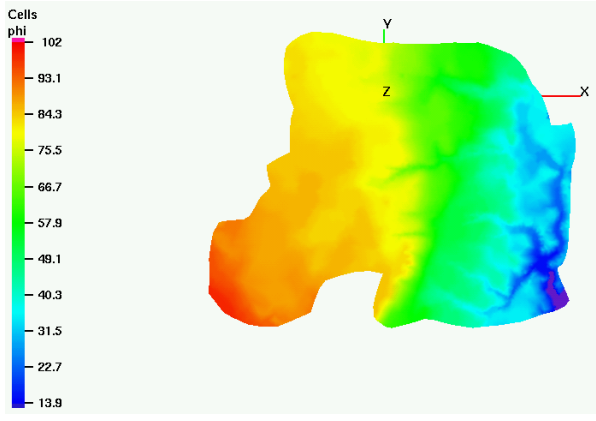

Figure 11: ϕ at $t = 0$.

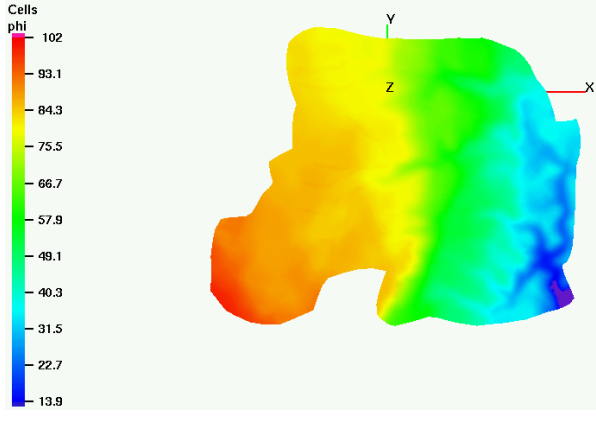

Figure 12: ϕ at $t = 60$ days.

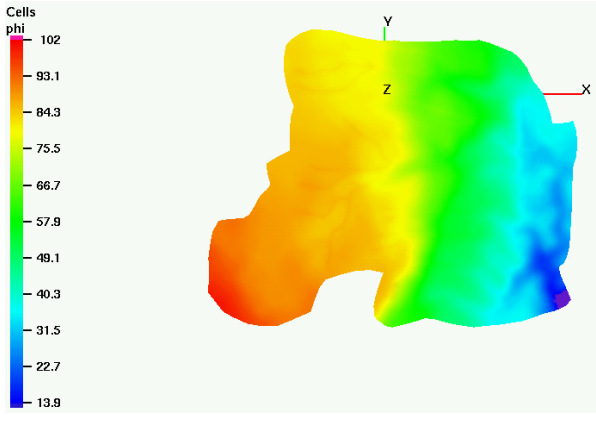

Figure 13: ϕ at $t = 180$ days.

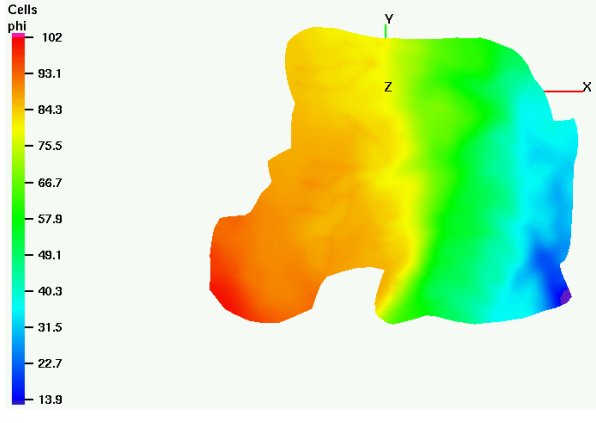

Figure 14: ϕ at $t = 330$ days.

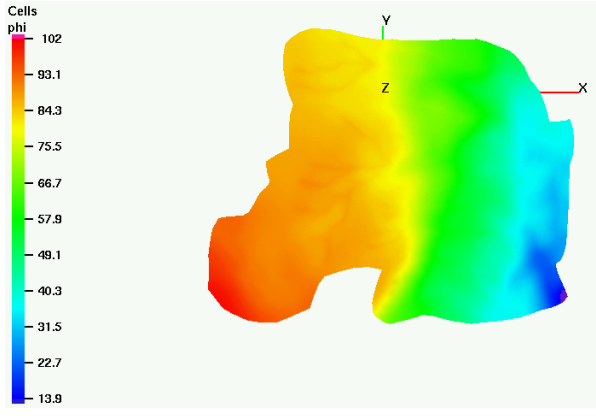

Figure 15: ϕ at $t = 420$ days.

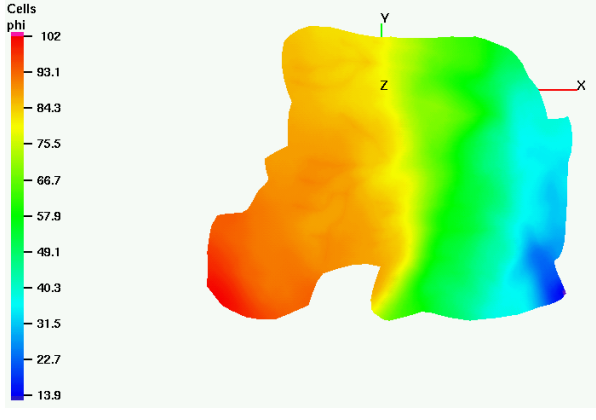

Figure 16: ϕ at $t = 540$ days.

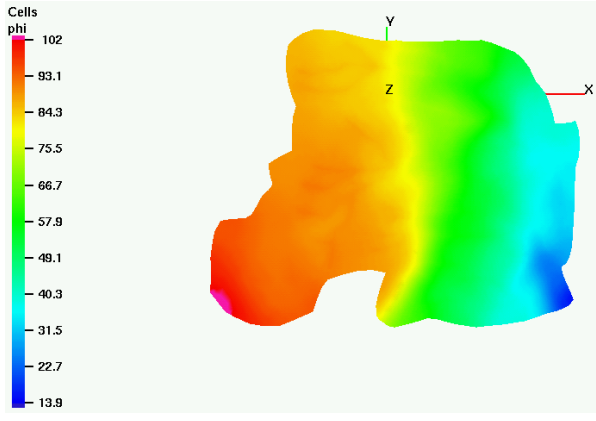

Figure 17: ϕ at $t = 690$ days.

5.2 Second case

The second example (results in figures 18 to 23) is a case with no raindrop and a constant recharge of 5 meters in upstream boundaries. Physical constants and initial state of aquifer freatic height level are holded. Resistivity coefficient for `stream_loss` element set is smaller than the first case in the scope to appreciate the recharge of the aquifer due to higher level of rivers.

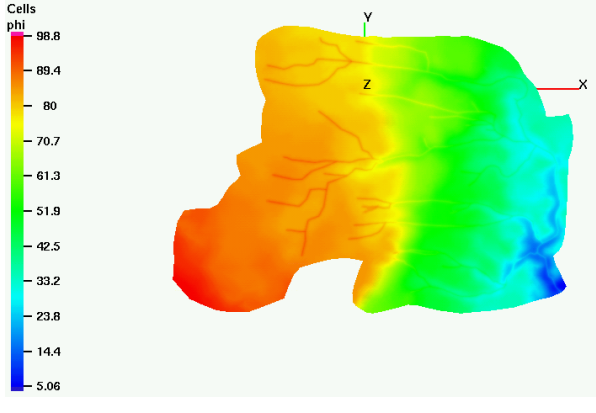

Figure 18: ϕ at $t = 0$.

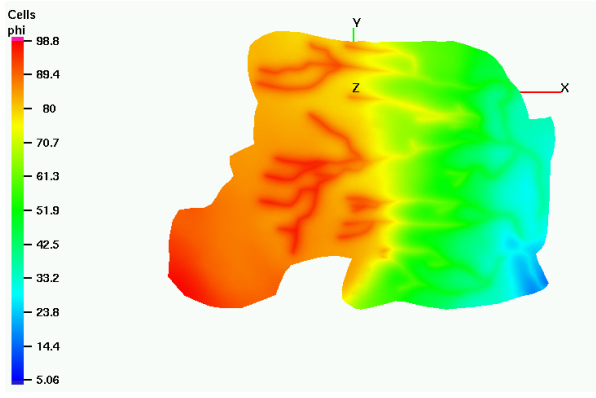

Figure 19: ϕ at $t = 200$ days.

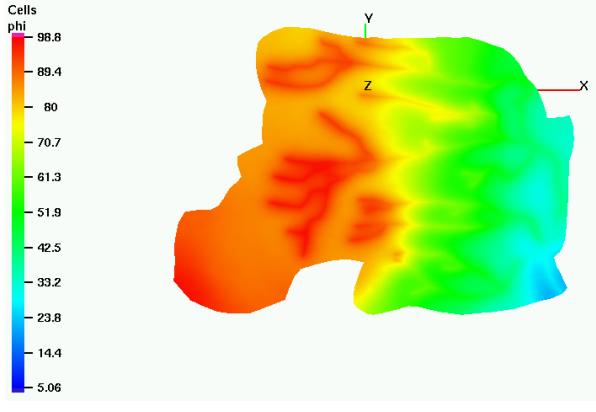

Figure 20: ϕ at $t = 400$ days.

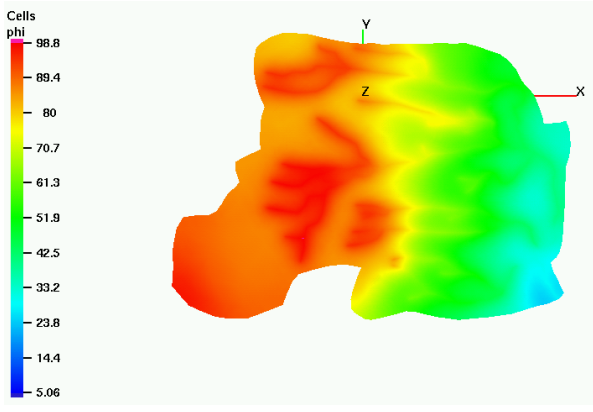

Figure 21: ϕ at $t = 600$ days.

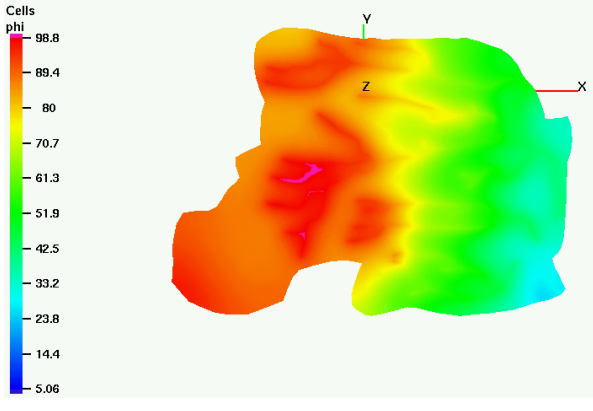

Figure 22: ϕ at $t = 800$ days.

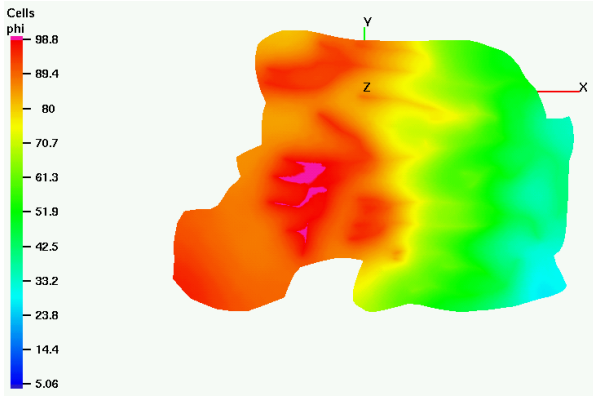

Figure 23: ϕ at $t = 1000$ days.

6 CONCLUSIONS

The primary goal of the present work was the development of a large scale hydrological model for surface and subsurface water flow.
More accurate physical data are being obtained through intensive measurements work. Future work includes a 2D Saint-Venant model for surface flow, multi-layers/multi-aquifer systems, pollutant transport.

ACKNOWLEDGMENT

This work has received financial support from *Consejo Nacional de Investigaciones Científicas y Técnicas* (CONICET, Argentina), *Agencia Nacional de Promoción Científica y Tecnológica* (ANPCyT) and *Universidad Nacional del Litoral* (UNL) through grants CONICET PIP 198/ *Germen-CFD*, SECyT-FONCyT-PICT-6973 *PROA* and CAI+D-UNL-PIP-02552-2000.
We made extensive use of freely distributed software as *Linux* OS, MPI, PETSc, Newmat, *GMV* and many others.

REFERENCES

[1] L. B. Rodriguez. *Investiagtion of Stream-Aquifer Interactions Using Coupled Surface-Water and Ground-Gater Flow Model. Phd. Thesis.* University of Arizona, (1995).
[2] INRIA Sophia Antipolis and community of researchers. *The CGAL Basic Library.* INRIA, (2002).
[3] R. Sibson. A brief description of natural neighbour interpolation. In V. Barnett, editor, *Interpreting Multivariate Data*, pages 21–36. John Wiley & Sons Ltd., (1981).

[4] N. Sukumar. *The Natural Element Method in Solid Mechanics. Phd. Thesis*. Northwestern University, Illinois, (1998).

[5] M. Storti, L. Dalcin, R. Paz, V. Sonzogni, and A. Yommi. An interface strip preconditioner for domain decomposition methods. In *First South-American Congress on Computational Mechanics - III Brazilian Congress on Computational Mechanics - VII Argentine Congress on Computational Mechanics*, (2002).

[6] Y. Saad. *Iterative Methods for Sparse Linear Systems*. PWS Publishing Co., (2000).

[7] C. Farhat and F.X. Roux. A method of finite element tearing and interconnecting and its parallel solution algorithm. *Int. J. Numer. Meth. Eng.*, **32**, 1205–1227 (1991).

[8] J. Mandel. Balancing domain decomposition. *Comm. Appl. Numer. Methods*, **9**, 233–241 (1993).

[9] P. Le Tallec and M. Vidrascu. Solving large scale structural problems on parallel computers using domain decomposition techniques. In M. Papadrakakis, editor, *Parallel Solution Methods in Computational Mechanics*, chapter 2, pages 49–85. John Wiley & Sons Ltd., (1997).

[10] C. Farhat and J. Mandel. The two-level FETI method for static and dynamic plate problems. *Comput. Methods Appl. Mech. Engrg.*, **155**, 129–152 (1998).